Langmuir

ARTICLE

pubs.acs.org/Langmuir

Assembly Kinetics of Nanocrystals via Peptide Hybridization

Urartu Ozgur Safak Seker,[*,†,∥] Gulis Zengin,[†] Candan Tamerler,[‡,§] Mehmet Sarikaya,[‡,§] and Hilmi Volkan Demir[*,†,∥]

[†]Department of Electrical and Electronics Engineering, Department of Physics and UNAM—Institute of Materials Science and Nanotechnology, Bilkent University, 06800 Ankara, Turkey

[‡]Molecular Biology and Genetics, MOBGAM, Istanbul Technical University, Maslak 34469, Istanbul, Turkey

[§]Genetically Engineered Materials Science and Engineering Center, Department of Materials Science and Engineering, University of Washington, Seattle, Washington 98105, United States

[∥]*Luminous!* Centre of Excellence for Semiconductor Lighting and Displays, School of Electrical and Electronic Engineering, Microelectronics Division, School of Physical and Mathematical Sciences, Physics and Applied Physics Division, Nanyang Technological University, 639798, Singapore

Supporting Information

ABSTRACT: The assembly kinetics of colloidal semiconductor quantum dots (QDs) on solid inorganic surfaces is of fundamental importance for implementation of their solid-state devices. Herein an inorganic binding peptide, silica binding QBP1, was utilized for the self-assembly of nanocrystal quantum dots on silica surface as a smart molecular linker. The QD binding kinetics was studied comparatively in three different cases: first, QD adsorption with no functionalization of substrate or QD surface; second, QD adsorption on QBP1-modified surface; and, finally, adsorption of QBP1-functionalized QD on silica surface. The surface modification of QDs with QBP1 enabled 79.3-fold enhancement in QD binding affinity, while modification of a silica surface with QBP1 led to only 3.3-fold enhancement. The fluorescence microscopy images also supported a coherent assembly with correspondingly increased binding affinity. Decoration of QDs with inorganic peptides was shown to increase the amount of surface-bound QDs dramatically compared to the conventional methods. These results offer new opportunities for the assembly of QDs on solid surfaces for future device applications.

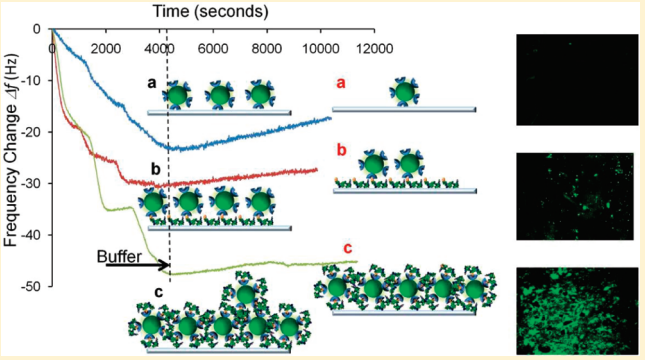

INTRODUCTION

Semiconductor colloidal quantum dots (QDs), also known as nanocrystals, have been widely exploited in numerous applications in physical and life sciences for their unique optical and electronic properties.[1−6] Immobilization of these quantum dots on solid inorganic surfaces is of fundamental importance for their optoelectronic device applications, including light-emitting diodes,[7] modulators,[8] photodetectors,[9] and photovoltaic devices,[10] and in their biomedical applications, including detection of pathogenic microorganisms[11] and imaging for biomedical applications.[12] In these applications, QDs are typically immobilized on surfaces using chemically assisted assembly techniques, which are based on covalent or noncovalent interactions such as organic[13,14] or inorganic templating,[15,16] self-assembled monolayers (SAMs),[17] electrostatic interactions,[18] and hydrogen bonding.[19] In addition to the chemical linker molecules, QDs can alternatively be embedded into a polymer matrix and coassembled onto the surface.[20] However, none of these approaches features specific binding. To devise a more controlled and robust QD immobilization technique, specific interactions between targeted substrate and QDs are needed. To cater this requirement, genetically engineered peptides for inorganics (GEPIs), which have been processed using combinatorial biology tools, namely, cells surface display[21] and phage display,[22,23] have been used as smart molecular linkers for specific self-assembly of QDs on various inorganic surfaces.

Inorganic material binding peptides have been screened and selected for metals,[24,25] metal oxides,[26,27] minerals,[28,29] and semiconductors.[30,31] Quantitative analysis of the interaction of such inorganic binding peptides with solid surfaces has been carried out to probe the binding kinetics and thermodynamics of inorganic binding peptides. Their interaction with substrates was tested using surface plasmon resonance spectroscopy (SPR),[32,33] quartz crystals microbalance with dissipation monitoring (QCM-D),[34,35] and atomic force microscopy (AFM).[36,37] These surface-sensitive

Received: December 13, 2010
Revised: February 13, 2011
Published: March 16, 2011

ACS Publications © 2011 American Chemical Society

techniques are key to real-time monitoring of the interaction of peptides with solid surfaces. The results from the binding experiments of inorganic binding peptides reveal a high affinity specific to the inorganic surface for which they are selected. The binding affinity of these peptides is comparable to those of biological molecular interaction and synthetic chemical linkers.[27] After a substantial analysis of the affinity and specificity of inorganic binding peptides for their binding affinity, studies were carried out toward utilization of these peptides. Employing the tools of genetic engineering, peptides were used for the targeted immobilization of specific proteins on inorganic surfaces for biosensing and bioassay applications.[38−41] Inorganic binding peptides were commonly utilized in applications for positioning of nanomaterials on solid surfaces and on multimaterial surfaces.[42−44] Utilization of the inorganic binding peptides also for building new nanoscale architectures was successfully demonstrated in previous studies. As a proof of concept study, the assembly of nanoparticles in a layer-by-layer assembly configuration was shown using inorganic peptides, e.g., titanium and silica binding peptides.[45,46] In a recent study, inorganic binding peptides expressed on the major coat protein of M13 viruses were used as a template to assemble nanomaterials to build a novel type of battery.[47] There are also a number of previous studies that have specifically used inorganic binding peptides for the assembly and patterning of nanocrystals on solid surfaces. For example, a gold binding peptide was utilized to immobilize QDs on a gold/platinum patterned silica surface with high selectivity.[48] Similarly, QDs were patterned on silica surface with high precision using the silica binding peptide QBP1.[49] Also, QD patterns in various shapes were created through the assembly of biotinylated peptides with dip pen nanolithography on a silica surface.[42] In another study, the QD assembly on gold surface was achieved with a specific gold binding peptide to control the emission intensity of the QD nanocrystals.[50] In all of these prior studies, however, the QDs and peptides have been immobilized sequentially on the solid substrate and the adsorption kinetics of QDs using peptide linkers have not been investigated to date.

Although there is an accumulating amount of research work being reported on the utilization of the semiconductor QD nanocrystals, only a limited number of studies have thus far investigated the kinetics of QD immobilization on solid surfaces. However, none of them has studied the QD adsorption kinetics using specific solid binding peptides as linkers till date. In this work, we present a study on the interaction of QDs with solid silica surface using silica binding QBP1 peptides as the linkers. QBP1 linker is a silica binding peptide that was obtained from a knowledge-based peptide design approach using bioinformatics tools. In this approach, a library of weak, moderate, and strong silica binders were used to extract the binding information from varying peptide sequences. Later, this information is used to create a function to produce silica binder with different affinities.[51,52] This study addresses how the peptides modify QD binding kinetics and how they should be utilized for the assembly of QDs on a technologically common substrate, silica surface. For that we explored and compared different assembly approaches to utilize QBP1 linkers for the enhanced binding of QDs on a silica surface.

In this study, we investigated three different cases to seek a more robust and controlled self-assembly technique for the immobilization of QDs on the silica surface. We used streptavidin-coated QDs (SA-QDs) and QBP1 biotinylated (QBP1-bio) at the N-terminus of the peptide to link QDs to peptides by exploiting the strong interaction between SA and biotin. In the first approach, we studied the binding kinetics of the SA-QDs on nonmodified silica surface. Second, we looked into the kinetics of SA-QD assemblies on modified silica surface that is furnished with silica-binding peptide (QBP1-bio). Finally, we monitored the binding kinetics of the peptide-functionalized QDs, namely, QBP1-bio-hybridized SA-QD (QBP1-bio-SA-QD) nanoassemblies, on nonmodified silica surface. We performed SPR spectroscopy and QCM-D-based analyses of the binding kinetics of these QDs and then supported these results with fluorescence microscopy measurements in each of three cases.

EXPERIMENTAL SECTION

Peptides and Buffers. We used a silica-binding peptide for the assembly experiments. The amino acid sequence of the peptide is PPPWLPYMPPWS. The peptide was synthesized by GeneScript using a solid-state peptide synthesis approach. The mass spectroscopy analysis yielded a 95% purity. The peptide was synthesized with a biotin group at its N- terminus. The biotin molecule was attached to the N-terminus of the peptide. The lyophilized peptide (QBP1-bio) was dissolved in phosphate-buffered saline (PBS) solution to obtain 10 μg/mL final peptide concentrations. PBS solution used in these experiments contains 200 mM NaCl, 45 mM Na_2CO_3, and 55 mM KH_2PO_4, and pH of the buffer was adjusted to 7.4.

Preperation of SA-QD−Biotin Conjugates and Experimental Sets. We used CdSe/ZnS core−shell semiconductor QDs conjugated with streptavidin purchased from Evident Technologies, Troy, NY. Their hydrodynamic size is around 25 nm in aqueous solution. They exhibit a peak emission wavelength at 520 nm.

We prepared the nanohybrids (QBP1-bio-SA-QD) by mixing 20 μL of bio-QBP1 (1 mg/mL) and SA coated QDs (2 μM) (SA-QD). The peptides were decorated through the interaction of the biotin end of the peptides with the streptavidin coating around the QDs. To remove the unbound peptides from the resulting nanohybrid solution, the final mixture was first adjusted to 250 μL with PBS and then filtered through a spin filter with a cutoff 10 kDa at 2000 rpm for 15 min. To ensure the removal of the retained free peptides, the nanohybrids were washed several times with PBS and spin-filtered. We further checked the quality of the formed nanohybrids by comparing their adhesion onto SA-coated quantum dots. Also, we observed a red shift in the photoluminescence of the peptide-conjugated SA-QDs compared to that of SA-coated QDs. The yield was not observed to be an issue when compared to the sequential assembly.

To study the binding kinetics of these QDs on silica substrates, we prepared three experimental sets for SPR, QCM-D, and fluorescence microscopy (FM) measurements; the details of the experimental setups are included in the instrumental sections. In the first set, we monitored the binding kinetics of SA-QD on nonmodified silica surface as a control group to distinguish the effect of QBP1-bio as a smart molecular linker in the self-assembly of SA-QDs. For the second set, we looked into the effect of using QBP1-bio-modified silica surface on the amount of adsorbed QDs. For this purpose we started with the decoration of the silica surface using this silica-binding peptide by flowing the peptide solution though a flow cell. Subsequently, we washed the surface with PBS solution to remove unbound or nonspecifically bound peptides from the silica surface. After the washing step, the silica surface was made ready for SA-QD immobilization, with free biotin ends of the peptides interacting with SA molecules. Through the interactions between the SA of SA-QDs and the biotin of the biotin-functionalized peptides, which are stationary on silica surface, QDs are adsorbed on silica surface. Next, the unbound and nonspecifically bound SA-QDs were detached from

the surface by washing with an excess of buffer solution. This experimental set is dubbed the sequential assembly sample, since the QD layer is sequentially assembled on top of the peptide layer. For the last experimental set, we examined the case where we hybridized QDs with peptides though SA−biotin interactions before immobilization on silica surface. Different from the second experimental set, we decorated SA-QDs instead of the silica surface with QBP1-bio. For this purpose, we combined SA-QD and QBP1-bio solutions under rigorous mixing before flowing though the silica surface. We optimized the concentrations and volumes so that QD surface is fully covered with peptide molecules. This last set is referred to as hybrid nanoassemblies. One of the most important properties of these hybrid nanoassemblies is their bifunctional characteristics. They serve two functions: first, they can specifically bind to a targeted inorganic surface; second, they are optically active.

Surface Plasmon Resonance (SPR) Studies. To monitor the binding kinetics of QDs we used a SPR spectroscopy instrument (Reichert Inc., Depew, NY). The instrument is equipped with a flow cell placed on a prism coupler of the device. SPR slides coated with 5 nm thick chromium and 50 nm thick gold were used as sensor surfaces. These gold-coated slides were finally coated with 10 nm thick silicon dioxide using a plasma-enhanced chemical vapor deposition system. The preparation of these slides was carried out as described in the Supporting Information of our previous study.[27] Slides were cleaned with a UV−ozone cleaner (Novoscan). The binding experiments were carried out at 25 °C. To establish a baseline, PBS buffer was flown on the SPR substrate. After the baseline was established, the solutions of QDs, peptides, or peptide−QD conjugates were pumped into the flow cell. After interacting with the silica surface, the loosely and nonspecifically bound QDs, peptides, or QD−peptide conjugates were removed from the surface by extensive washing. The desorption curve when changing from QD solution to PBS indicated a negligible amount of bulk shift effect; the interaction had a very limited desorption. The binding kinetics of the interacting species was tracked in real-time with the software supplied with the instrument.

Quartz Crystal Microbalance-Dissipation (QCM-D) Studies. The adsorption behavior of QDs was monitored using a quartz crystal microbalance (Q-Sense E1, Q-Sense Co., Frolunda, Sweden). All of the peptide solution and QD solutions were prepared as mentioned above. We carried QCM-D measurements for the three different cases. We used a silica-coated sensor, also from Q-Sense. The assembly of each layer was carried out using a peristaltic pump at a flow rate of 10 μL/min at 25 °C. After each run, the sensor surface was flushed with buffer to remove nonspecifically and weakly bound materials. We gathered the frequency change data using the software supplied along with the instrument.

Fluorescence Microscopy Studies. We further analyzed the QD-assembled SPR slides using confocal microscopy (LSM510 DuoScan, Carl Zeiss, Thornwood, NY).

RESULTS AND DISCUSSION

The adsorption of QDs was studied in three different configurations: SA-QDs on nonmodified silica surface, SA-QDs on peptide-modified silica surface, and peptide-hybridized SA-QDs on nonmodified silica surface. The first step of adsorption experiments was completed using surface plasmon resonance spectroscopy. The data gathered from the SPR experiments were fitted to a Langmuir adsorption model. In Figure 1a−c the adsorption sensograms of SA-QDs corresponding to these three different cases are given. In these adsorption sensograms, the shift in the SPR wavelength results from the change in the refractive index, which therefore reflects the amount of dry mass adsorbed on an average area.[53,54]

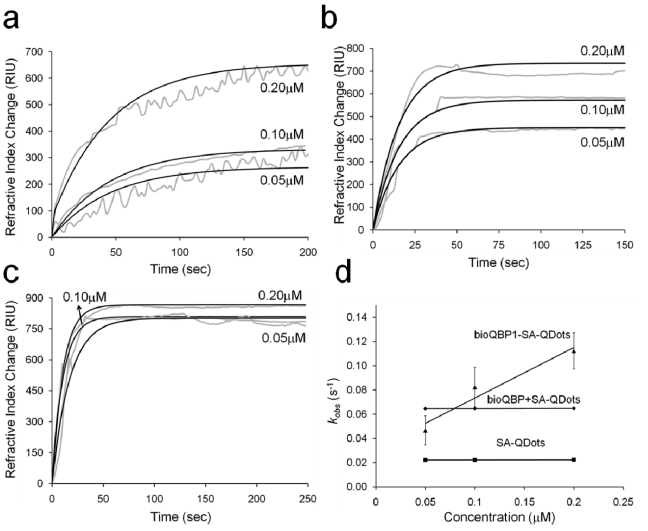

Figure 1. Surface plasmon resonance refractive index change as a function of time for QD adsorption onto silica surface in the case where (a) SA-QDs are immobilized on nonmodified silica surface (control group), (b) SA-QDs are immobilized on silica binding peptide modified (QBP1-bio) silica surface (sequential assembly approach), and (c) hybrid nanoassemblies (SA-QDs hybridized with silica-binding peptides before interacting with the surface) are immobilized on nonmodified silica surface. The adsorption rate is given as a function of SA-QD concentration in part d.

Table 1. Adsorption Equilibrium Constants and Binding Free Energies of SA-QDs on Silica Surface, for Three Different Experimental Sets

kinetic constant	SA-QD	sequential assembly	nanohybrid assembly
k_a (M^{-1}/s)	0.60×10^3	5.39×10^3	4.66×10^4
k_d (s^{-1})	2.20×10^{-2}	6.40×10^{-2}	2.30×10^{-2}
K_{eq} (M^{-1})	2.56×10^4	8.43×10^4	2.03×10^6
ΔG (kcal mol^{-1})	−5.9	−6.7	−8.6

The SPR wavelength shift increases from part a to part c in Figure 1. The maximum shift was monitored in Figure 1c for the case of peptide-hybridized SA-QD adsorption on silica surface, which implies a maximum adsorbed QD mass on the silica surface among all cases. In Figure 1a, for the control group, even though peptide linkers were used neither on the silica surface nor on SA-QD surface, SA-QDs are adsorbed on silica surface to some degree due to some nonspecific interactions between SA and the silica surface; in particular, hydrophilic interactions may dominate. In Figure 1b, with the use of QBP1-bio immobilized on the silica surface, more SA-QDs are adsorbed on the silica surface via the supramolecular interaction between biotin and SA. However, there are some limitations in such sequential assembly of QDs on peptide-modified silica surface due to the diffusion effects during the adsorption.[55,56] This triggers problems with the availability of the surface-bound biotin molecules. Furthermore, the mass transfer of SA-QDs is diffusion-limited since for adsorption they have to interact with the immobile biotin part of the peptides, which are also stuck on the silica surface. In fact, for stronger adsorption, SA-QDs have to interact with QBP1-bio on the surface, which is less probable compared to the interaction of SA and biotin molecules in solution (under mixing). Therefore,

formation of the QBP1-bio-SA-QD hybrid nanoassemblies before immobilization offers a solution to significantly improve the SA-QD adsorption.

Moreover, the Langmuir model fitted to actual data points are given in Figure 1d, where the apparent adsorption rate is recorded as a function of SA-QD concentration. The adsorption equilibrium constants and the change in the Gibbs free energy for binding process were calculated from the SPR data for each case. As given in Table 1, the adsorption equilibrium constant increases when using silica-binding peptide QBP1-bio as a smart molecular linker. Using sequential assembly leads to ~3.3-fold enhancement in the adsorption equilibrium constant compared to the control group, in which SA-QDs were only immobilized on nonmodified silica surface. This increase in equilibrium adsorption rate points out a clear improvement in the binding affinity of the SA-QDs on silica surface. This is favored by the specific interaction of the SA molecules with the surface-bound biotin molecules, which are bound to the silica surface through the specific interaction of the silica-binding peptide with the silica. In this approach, there are two possible dominating effects determining the amount of SA-QD adsorption on peptide modified silica surface. The first effect comes from the amount of QBP1-bio adsorption on silica surface, since for the SA-QD adsorption the silica surface must have been sufficiently covered with peptides. The previous studies showed that the bound QBP1-bio has a surface coverage of 80% on the silica surface.[49] Second, noting that the interaction between SA and biotin is one of the strongest known in nature, it definitely influences the SA-QD adsorption on silica surface. However, these two effects are not the only influences on SA-QD adsorption, because the interaction of the biotin molecule with the active site of SA is restricted by the mass transfer problem of SA-QDs on the stationary biotin ends of the bound peptides.

To improve the binding of the SA-QDs on the silica surface, the hybrid nanoassemblies were formed by filling the available sites on SA on the outer shell of SA-QD with biotins while rigorously mixing in solution so that SA-QD surface was fully hybridized and saturated with the silica-binding peptides. These new hybrid nanoassemblies have an enhanced capability to assemble on silica surface in a more controlled and robust manner. Compared to the control group, where the SA-QDs were immobilized on the nonmodified surface, a 79.3-fold enhancement in the binding affinity was achieved with these hybrid nanoassemblies. However, the binding interaction of streptavidin directly with surface immobilized biotin available in the literature has a lower dissociation rate constant, which is 4×10^{-6} s^{-1}, compared to the dissociation constant for the interaction of streptavidin-coated QDs with surface-immobilized peptide obtained in this study, which is 6.4×10^{-2} s^{-1}.[57,58] This difference may arise due to the steric hindrance that occurred during the interaction of streptavidin-coated QDs with surface-bound biotin in the case of sequential assembly. Also, one should keep in mind that the mode of interaction of streptavidin conjugates with surface-bound biotin is expected to be looser compared to the interaction of wild-type streptavidin, possibly because of molecular crowding and mass transport limitation, as well as a structural rearrangement of streptavidin upon conjugation.

The kinetic constants listed in Table 1 are important for the comparison of these different ways of attaching QDs on a given solid surface. When we compare the adsorption rates, k_a, for QDs from the silica surfaces following the assembly, the adsorption of

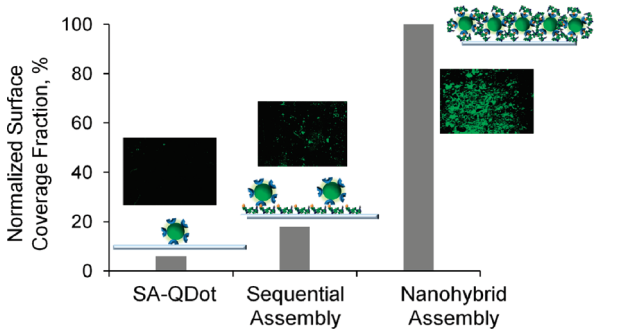

Figure 2. Relative surface coverage of (a) the control group, where SA-QDs are immobilized on nonmodified silica surface; (b) the sequential assemblies, where SA-QDs are immobilized on silica binding peptide-mediated silica surface; and (c) the hybrid nanoassemblies, where SA−QDs are hybridized with silica-binding peptide before immobilization onto the silica surface, using SPR and fluorescence microscopy data.

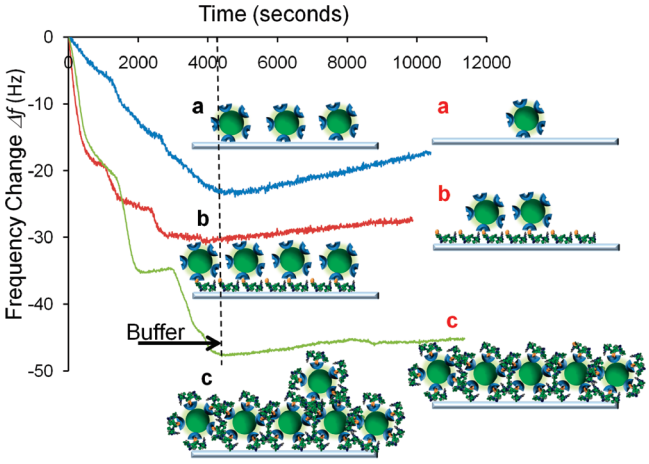

Figure 3. QCM-D real-time monitoring of the binding of SA-QDs for (a) the control set, (b) the sequential assembly set, and (c) the hybrid nanoassembly set on silica surface.

SA-QDs is faster in the case of using peptides as linker molecules. This observation makes the point about the effectiveness of the QBP1 peptide in the assembly of QDs. On the other hand, when the peptides are decorated around the SA-QDs and the hybrid nanoassemblies are formed, the adsorption rate is increased dramatically by almost 77.2 times. In Table 1, the calculated Gibbs free energies for three different QD binding approaches are presented. For hybrid nanoassemblies, the Gibbs free energy is minimum, which means that this system is thermodynamically more stable than both the sequential assembly set and the control group, since this process can take place without intervention of external forces and yields a lower Gibbs free energy for QD adsorption.

The surface coverage of QDs was also calculated using the binding isotherms (see Supporting Information). The calculated surface coverage values were normalized with the surface coverage of hybrid nanoassemblies (QBP1-bio-SA-QDs), since the highest adsorption and surface coverage of SA-QDs were obtained in the case of the hybrid nanoassemblies. The surface coverage fraction for bioQBP1-SA-QD was kept at 100% while others were normalized. The normalized surface coverage for each case is given in Figure 2, coupled with schematics representing

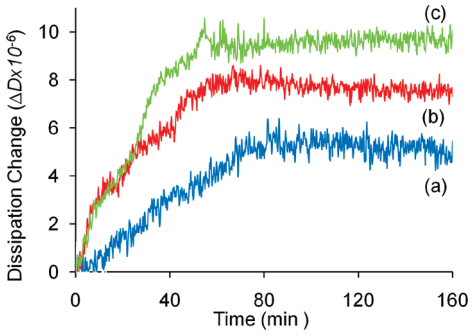

Figure 4. Dissipation change for (a) the control set, (b) the sequential assembly set, and (c) the hybrid nanoassembly set on silica surface.

adsorbed SA-QDs and fluorescence microscopy images of the resulting SPR slides with 0.25 μM SA-QD concentration. The fluorescence microscopy images also support SPR data and adsorption results as well as the surface coverage percentages. The gradual increase in the brightness of fluorescence microscopy images from the control group to the hybrid nanoassemblies implies a direct correlation between the surface coverage of the SA-QDs and total luminescence of the adsorbed SA-QDs.

We further verified the adsorption behavior of the SA-QDs on a silica surface in three experimental sets using a QCM-D system, which is another powerful technique for real-time monitoring of molecular interactions. The frequency shifts and dissipation changes recorded in QCM-D measurements are shown in Figures 3 and 4, respectively. Both of the variables are good indicators of the quality of the film formed and the enhancement of the adsorbed QDs on the surface caused by the peptide hybridization of SA-QDs. One should note that QCM-D is basically a gravimetric method, and the frequency shift in Figure 3 supports the idea that the amount of QDs assembled on silica in the hybrid case is higher compared to the SA-QDs adsorbed on silica in other combinations.

Even though SPR and QCM-D can be interchangeably used to study adsorption kinetics of molecules, in fact, they provide different information about molecular interactions. For instance, while SPR gives an idea about the film thickness and deposited dry mass by measuring the change in the refractive index, QCM-D can also monitor the dissipation of the film deposited on the sensor crystal by recording data at different overtones.[59,60] This change in the dissipation of the film gives direct information about the amount of water held by the molecules in the system, which is not possible to detect in SPR measurements.[35] It is also reported that the entrapment of the water molecules is related to the surface coverage. At higher surface coverage levels, molecules are expected to be more dissipative, as a result of the entrapment of the large amount of water on the sensor surface. QCM-D results revealed that the change in the dissipation is a maximum in the hybrid nanoassemblies and it is a minimum in the control group. However, compared to the shifts in resonance frequency in each case, the change in the dissipation for hybrid assemblies is smaller than expected in Figure 3. From SPR results and fluorescence microscopy images, we know that the surface coverage is larger in the case of the hybrid nanoassemblies. Therefore, we would expect the change in the dissipation of hybrid assemblies to be correspondingly larger compared to the dissipation change we observed in this study for the other two cases, as a higher surface coverage leads to more water entrapment. But this not the case; so, this experimental observation indicates that the film of the hybrid nanoassemblies is condensed and, in contrast to high surface coverage, the densely packed hybrid nanoassemblies do not hold a large amount of water.

CONCLUSION

The self-assembly process is a well-established tool to create ordered nanostructures for applications in physical and life sciences. One of the challenges is to build and control these systems by means of molecular recognition for more robust and specific processes. The biological molecules and systems include many of the samples of the self-assembled systems. Herein, we exploit a combinatorial biology selected peptide, which is capable of specifically binding to silica surface. We utilized this peptide as a smart molecular linker for the controlled assembly of the SA-QDs on silica surface, in the process of self-assembly. We investigated the binding kinetics of SA-QDs on a silica surface using different approaches. Hybridization of SA-QDs with QBP1-bio enhanced the binding of SA-QDs on the silica surface. These hybrid nanoassemblies have been found to have a higher surface coverage compared to the assembly of SA-QDs on the silica surface and the assembly of SA-QDs on QBP1-bio-decorated surface. We observed that the hybrid nanoassemblies are attached to the silica surface at a higher affinity and the formed film on the silica surface is more densely assembled compared to other cases.

This quantitative study proposes the first account of utilizing inorganic binding peptides to increase the adsorption of the quantum dots on a given solid surface. Not only is using a linker molecule important for a better assembly of nanomaterials but also the way of decorating the linker molecule is critical for better functionality of the nanomaterials. Understanding the adsorption behavior of such nanoassemblies is crucial to controlling and constructing new devices with improved functionality.

ASSOCIATED CONTENT

Supporting Information. Details of the calculation of the binding kinetics constants and surface coverage of SA-QDs from SPR experiments and a desorption curve for SPR data. This material is available free of charge via the Internet at http://pubs.acs.org.

AUTHOR INFORMATION

Corresponding Author

*U.O.S.S: phone, [+90] (312) 2901021; fax, [+90] (312) 2901123; e-mail, uosseker@ntu.edu.sg. H.V.D.: phone, [+65] 67905395; e-mail, hvdemir@ntu.edu.sg, volkan@bilkent.edu.tr

ACKNOWLEDGMENT

We acknowledge the financial support of ESF European Young Investigator Award (EURYI) Program and TUBITAK under the Grant No. EEEAG 107E088, 109E002, 109E004, 110E010, and 110E156; of NSF-MRSEC (GEMSEC) and NSF BioMat programs at UW; and of TUBITAK/NSF IRES ITU/UW Joint Project (107T250) (C.T. and M.S.). H.V.D. acknowledges additional support from the Turkish National Academy of Sciences Distinguished Young Scientist Award, TUBA GEBIP, and Singapore NRF-RF-2009-09.

REFERENCES

(1) Medintz, I. L.; Clapp, A. R.; Brunel, F. M.; Tiefenbrunn, T.; Uyeda, H. T.; Chang, E. L.; Deschamps, J. R.; Dawson, P. E.; Mattoussi, H. *Nat. Mater.* **2006**, *5* (7), 581–589.

(2) Sapsford, K. E.; Pons, T.; Medintz, I. L.; Mattoussi, H. *Sensors* **2006**, *6* (8), 925–953.

(3) Ferry, D. K.; Bird, J. P.; Akis, R. *Physica E* **2004**, *25* (2−3), 298–302.

(4) Korbutyak, D. V.; Kalytchuk, S. M.; Geru, I. I. *J. Nanoelectron. Optoelectron.* **2009**, *4* (1), 174–179.

(5) Talapin, D. V.; Murray, C. B. *Science* **2005**, *310* (5745), 86–89.

(6) Sambur, J. B.; Novet, T.; Parkinson, B. A. *Science* **2010**, *330* (6000), 63–66.

(7) Nizamoglu, S.; Ozel, T.; Sari, E.; Demir, H. V. *Nanotechnology* **2007**, *18* (6), 075401.

(8) Majumdar, A.; Manquest, N.; Faraon, A.; Vuckovic, J. *Opt. Express* **2010**, *18* (5), 3974–3984.

(9) Konstantatos, G.; Howard, I.; Fischer, A.; Hoogland, S.; Clifford, J.; Klem, E.; Levina, L.; Sargent, E. H. *Nature* **2006**, *442* (7099), 180–183.

(10) Bang, J. H.; Kamat, P. V. CdSe and CdTe. *ACS Nano* **2009**, *3* (6), 1467–1476.

(11) Yang, L. J.; Li, Y. B. *Analyst* **2006**, *131* (3), 394–401.

(12) Medintz, I. L.; Uyeda, H. T.; Goldman, E. R.; Mattoussi, H. *Nat. Mater.* **2005**, *4* (6), 435–446.

(13) Braun, P. V.; Osenar, P.; Tohver, V.; Kennedy, S. B.; Stupp, S. I. *J. Am. Chem. Soc.* **1999**, *121* (32), 7302–7309.

(14) Hwang, S. H.; Moorefield, C. N.; Wang, P. S.; Jeong, K. U.; Cheng, S. Z. D.; Kotta, K. K.; Newkome, G. R. *J. Am. Chem. Soc.* **2006**, *128* (23), 7505–7509.

(15) Dais, C.; Mussler, G.; Sigg, H.; Fromherz, T.; Auzelyte, V.; Solak, H. H.; Grutzmacher, D. *Europhys. Lett.* **2008**, *84* (6), 67017.

(16) Yakes, M. K.; Cress, C. D.; Tischler, J. G.; Bracker, A. S. *ACS Nano* **2010**, *4* (7), 3877–3882.

(17) Gupta, S.; Uhlmann, P.; Agrawal, M.; Lesnyak, V.; Gaponik, N.; Simon, F.; Stamm, M.; Eychmuller, A. *J. Mater. Chem.* **2008**, *18* (2), 214–220.

(18) Tang, Z. Y.; Zhang, Z. L.; Wang, Y.; Glotzer, S. C.; Kotov, N. A. *Science* **2006**, *314* (5797), 274–278.

(19) Komarala, V. K.; Rakovich, Y. P.; Bradley, A. L.; Byrne, S. J.; Corr, S. A.; Gun'ko, Y. K. *Nanotechnology* **2006**, *17* (16), 4117–4122.

(20) Li, S.; Toprak, M. S.; Jo, Y. S.; Dobson, J.; Kim, D. K.; Muhammed, M. *Adv. Mater.* **2007**, *19* (24), 4347.

(21) Hnilova, M.; Oren, E. E.; Seker, U. O. S.; Wilson, B. R.; Collino, S.; Evans, J. S.; Tamerler, C.; Sarikaya, M. *Langmuir* **2008**, *24* (21), 12440–12445.

(22) Smith, G. P. *Science* **1985**, *228* (4705), 1315–1317.

(23) Sarikaya, M.; Tamerler, C.; Jen, A. K. Y.; Schulten, K.; Baneyx, F. *Nat. Mater.* **2003**, *2* (9), 577–585.

(24) Naik, R. R.; Stringer, S. J.; Agarwal, G.; Jones, S. E.; Stone, M. O. *Nat. Mater.* **2002**, *1* (3), 169–72.

(25) Brown, S.; Sarikaya, M.; Johnson, E. *J. Mol. Biol.* **2000**, *299* (3), 725–35.

(26) Sano, K. I.; Sasaki, H.; Shiba, K. *Langmuir* **2005**, *21* (7), 3090–3095.

(27) Seker, U. O.; Wilson, B.; Sahin, D.; Tamerler, C.; Sarikaya, M. *Biomacromolecules* **2009**, *10* (2), 250–7.

(28) Gungormus, M.; Fong, H.; Kim, I. W.; Evans, J. S.; Tamerler, C.; Sarikaya, M. *Biomacromolecules* **2008**, *9* (3), 966–73.

(29) Donatan, S.; Yazici, H.; Bermek, H.; Sarikaya, M.; Tamerler, C.; Urgen, M. *Mater. Sci. Eng., C* **2009**, *29* (1), 14–19.

(30) Whaley, S. R.; English, D. S.; Hu, E. L.; Barbara, P. F.; Belcher, A. M. *Nature* **2000**, *405* (6787), 665–668.

(31) Estephan, E.; Larroque, C.; Cuisinier, F. J. G.; Balint, Z.; Gergely, C. *J. Phys. Chem. B* **2008**, *112* (29), 8799–8805.

(32) Seker, U. O. S.; Wilson, B.; Dincer, S.; Kim, I. W.; Oren, E. E.; Evans, J. S.; Tamerler, C.; Sarikaya, M. *Langmuir* **2007**, *23* (15), 7895–7900.

(33) Tamerler, C.; Oren, E. E.; Duman, M.; Venkatasubramanian, E.; Sarikaya, M. *Langmuir* **2006**, *22* (18), 7712–8.

(34) Ishikawa, K.; Yamada, K.; Kumagai, S.; Sano, K. I.; Shiba, K.; Yamashita, I.; Kobayashi, M. *Appl Phys Express* **2008**, *1* (3), 034006.

(35) Chen, H. B.; Su, X. D.; Neoh, K. G.; Choe, W. S. *Anal. Chem.* **2006**, *78* (14), 4872–4879.

(36) Hayashi, T.; Sano, K.; Shiba, K.; Kumashiro, Y.; Iwahori, K.; Yamashita, I.; Hara, M. *Nano Lett* **2006**, *6* (3), 515–9.

(37) So, C. R.; Tamerler, C.; Sarikaya, M. *Angew. Chem., Int. Ed.* **2009**, *48* (28), 5174–7.

(38) Park, T. J.; Zheng, S.; Kang, Y. J.; Lee, S. Y. *FEMS Microbiol. Lett.* **2009**, *293* (1), 141–147.

(39) Park, T. J.; Lee, S. Y.; Lee, S. J.; Park, J. P.; Yang, K. S.; Lee, K. B.; Ko, S.; Park, J. B.; Kim, T.; Kim, S. K.; Shin, Y. B.; Chung, B. H.; Ku, S. J.; Kim, D. H.; Choi, I. S. *Anal. Chem.* **2006**, *78* (20), 7197–7205.

(40) Zheng, S.; Kim, D. K.; Park, T. J.; Lee, S. J.; Lee, S. Y. *Talanta* **2010**, *82* (2), 803–809.

(41) Woodbury, R. G.; Wendin, C.; Clendenning, J.; Melendez, J.; Elkind, J.; Bartholomew, D.; Brown, S.; Furlong, C. E. *Biosens. Bioelectron.* **1998**, *13* (10), 1117–1126.

(42) Wei, J. H.; Kacar, T.; Tamerler, C.; Sarikaya, M.; Ginger, D. S. *Small* **2009**, *5* (6), 689–693.

(43) Tamerler, C.; Duman, M.; Oren, E. E.; Gungormus, M.; Xiong, X. R.; Kacar, T.; Parviz, B. A.; Sarikaya, M. *Small* **2006**, *2* (11), 1372–1378.

(44) Matsukawa, N.; Nishio, K.; Sano, K.; Shiba, K.; Yamashita, I. *Langmuir* **2009**, *25* (6), 3327–3330.

(45) Sano, K.; Yoshii, S.; Yamashita, I.; Shiba, K. *Nano Lett* **2007**, *7* (10), 3200–2.

(46) Sano, K.; Sasaki, H.; Shiba, K. *J. Am. Chem. Soc.* **2006**, *128* (5), 1717–22.

(47) Lee, Y. J.; Yi, H.; Kim, W. J.; Kang, K.; Yun, D. S.; Strano, M. S.; Ceder, G.; Belcher, A. M. *Science* **2009**, *324* (5930), 1051–5.

(48) Tamerler, C.; Duman, M.; Oren, E. E.; Gungormus, M.; Xiong, X.; Kacar, T.; Parviz, B. A.; Sarikaya, M. *Small* **2006**, *2* (11), 1372–8.

(49) Kacar, T.; Ray, J.; Gungormus, M.; Oren, E. E.; Tamerler, C.; Sarikaya, M. *Adv. Mater.* **2009**, *21* (3), 295–299.

(50) Zin, M. T.; Munro, A. M.; Gungormus, M.; Wong, N. Y.; Ma, H.; Tamerler, C.; Ginger, D. S.; Sarikaya, M.; Jen, A. K. Y. *J. Mater. Chem.* **2007**, *17* (9), 866–872.

(51) Oren, E. E.; Tamerler, C.; Sahin, D.; Hnilova, M.; Seker, U. O.; Sarikaya, M.; Samudrala, R. *Bioinformatics* **2007**, *23* (21), 2816–22.

(52) Oren, E. E.; Notman, R.; Kim, I. W.; Evans, J. S.; Walsh, T. R.; Samudrala, R.; Tamerler, C.; Sarikaya, M. *Langmuir* **2010**, *26* (13), 11003–11009.

(53) Reimhult, E.; Larsson, C.; Kasemo, B.; Hook, F. *Anal. Chem.* **2004**, *76* (24), 7211–7220.

(54) Jung, L. S.; Campbell, C. T.; Chinowsky, T. M.; Mar, M. N.; Yee, S. S. *Langmuir* **1998**, *14* (19), 5636–5648.

(55) So, C. R.; Tamerler, C.; Sarikaya, M. *Angew. Chem., Int. Ed.* **2009**, *48* (28), 5174–5177.

(56) Hyre, D. E.; Le Trong, I.; Merritt, E. A.; Eccleston, J. F.; Green, N. M.; Stenkamp, R. E.; Stayton, P. S. *Protein Sci.* **2006**, *15* (3), 459–467.

(57) Jung, L. S.; Nelson, K. E.; Stayton, P. S.; Campbell, C. T. *Langmuir* **2000**, *16* (24), 9421–9432.

(58) Jung, L. S.; Nelson, K. E.; Campbell, C. T.; Stayton, P. S.; Yee, S. S.; Perez-Luna, V.; Lopez, G. P. *Sens. Actuator B* **1999**, *54* (1−2), 137–144.

(59) Hook, F.; Kasemo, B.; Nylander, T.; Fant, C.; Sott, K.; Elwing, H. *Anal. Chem.* **2001**, *73* (24), 5796–5804.

(60) Janshoff, A.; Galla, H. J.; Steinem, C. *Angew. Chem., Int. Ed.* **2000**, *39* (22), 4004–4032.